IEEE Access
Multidisciplinary | Rapid Review | Open Access Journal

Received January 22, 2019, accepted February 12, 2019, date of publication February 26, 2019, date of current version March 8, 2019.

Digital Object Identifier 10.1109/ACCESS.2019.2900729

Experimental Phase Separation Differential Chaos Shift Keying Wireless Communication Based on Matched Filter

CHAO BAI[1], HAI-PENG REN[1], (Member, IEEE), AND CELSO GREBOGI[1,2]
[1]Shaanxi Key Laboratory of Complex System Control and Intelligent Information Processing, Xi'an University of Technology, Xi'an 710048, China
[2]Institute for Complex Systems and Mathematical Biology, University of Aberdeen, Aberdeen AB24 3UE, U.K.

Corresponding author: Hai-Peng Ren (renhaipeng@xaut.edu.cn)

This work was supported in part by the National Natural Science Foundation of China under Grant 61172070, in part by the Scientific and Technological Innovation Leading Talents Program of Shaanxi Province, and in part by the Key Basic Research Fund of Shaanxi Province under Grant 2016ZDJC-01. The work of C. Bai was supported by the Excellent Ph.D. Research Fund (310-252071603) at XAUT.

ABSTRACT New findings have been identified recently for chaos application in communication systems, including the simplest matched filter to maximize the signal-to-noise ratio (SNR) and the ability to resist multi-path propagation. However, chaos has a broad band frequency spectrum, which impedes its application in the conventional wireless communication systems due to the antenna and transducer bandwidth. To deal with such problem, the chaos generated by a second order hybrid system (SOHS) with a fixed basis function is used for Differential Chaos Shift Keying (DCSK) communication. A sinusoidal and its orthogonal signal are used to separate the reference signal and the information bearing signal, which are transmitted in the wireless channel. In such a way, the obstacle to broadband signal transmission in a wireless channel is overcome. A matched filter, using the convolution of the received signal and the time reverse of the basis function, maximizes the SNR at the receiver. Moreover, the proposed SOHS-DCSK provides an additional bitstream due to the chaotic signal generated by the SOHS, being capable to encode information as well. The two information sub-streams can be transmitted simultaneously in the proposed method, which possesses different bit transmission rates and reliability. In this way, the High Priority (HP) information bits are transmitted at a low transmission rate, while the Low Priority (LP) information bits are transmitted at a higher transmission rate. Hence, the proposed SOHS-DCSK method not only provides a higher data transmission rate as compared to the conventional DCSK but also makes the transmitted signal to be compatible with the conventional transducer and antenna. Due to the matched filter used, the proposed method achieves a lower bit error rate of the HP information as compared to the other existing enhanced DCSK variants for both additive white Gaussian noise channel and wireless communication channel. The numerical simulations and experiments based on the wireless open-access research platform show the validity and superiority of the proposed method.

INDEX TERMS Chaotic shape forming filter, matched filter, DCSK, wireless communication.

I. INTRODUCTION

Since Hayes *et.al*. argued in 1993 that chaotic signals can be used in communication systems [1], [2], the continuous efforts [3]–[5] are resulting in the successful application to the commercial wired fiber-optic channel [6]. The motivation to apply chaos in communication lies in the significant advantages provided by the chaotic signals, such as the large channel capacity brought by broadband spectrum [7], increased transmission security due to noise-like waveform [8], delta-function-like autocorrelation property required by spread spectrum systems [9], [10], and resistance to multipath propagation owning to chaos properties [11], [12].

In the past two decades, many digital chaos-based communication systems have been suggested, and the major efforts have focused on the non-coherent communication systems. Non-coherent communication avoids the chaotic synchronization, which is hard to achieve when the received signal is seriously distorted by the communication channel.

The associate editor coordinating the review of this manuscript and approving it for publication was Shuai Han.

The typical non-coherent communication system is the Differential Chaos Shift Keying (DCSK) [13] and its constant power version Frequency Modulated DCSK (FM-DCSK) [14], the FM-DCSK has already been included in the latest international standard for Wireless Body Area Networks (WBANs), see, IEEE 802.15.6 [15]. These methods transmit the reference signal and information bearing signal successively, so that they undergo the same channel distortion, which makes the communication systems to exhibit strong robustness to channel distortions, and to achieve low bit error rate (BER) in complex communication channels. The demodulation is carried out without the channel estimation, which simplifies the decoding algorithm, especially for low-cost, low-power and low-complexity Wireless Personal Area Networks (WPAN) and for Wireless Sensor Networks (WSN) applications [16], [17]. In addition, a Noise Reduction DCSK (NR-DCSK) system is presented in [18] to further enhance system performance, where the chaotic signal samples are duplicated p times in the carrier signal. The average operation at the receiver acts as a filter to reduce the effect of noise, which decreases the BER significantly as compared to the conventional DCSK and FM-DCSK. However, the drawbacks of all such methods are the low data transmission rate and the use of wideband delay units, which are difficult to implement in the current Complementary Metal Oxide Semiconductor (CMOS) technology [19]. In [20], a High Efficiency DCSK (HE-DCSK) is proposed to achieve double bit transmission rate and slightly better BER as compared to the conventional DCSK method. However, it requires more delay units in the system configuration, which increases the complexity of device implementation. In [21], a Reference-Modulated DCSK (RM-DCSK) is proposed to reduce the number of delay units required by HE-DCSK, which achieves similar BER and data transmission rate to that of the HE-DCSK. Moreover, [22]–[24] either considered the orthogonality of Walsh code sequence or designed orthogonal chaotic basis signals to transmit multi-bits simultaneously, which improved the spectral efficiency and the data transmission rate, effectively. However, the orthogonality is destroyed in the wireless channel, which restricts the application of those methods. Reference [25] proposes an Improved DCSK (I-DCSK) to avoid the usage of delay units, which achieves double bit transmission rate and lower BER as compared to the conventional DCSK. The drawback of I-DCSK is its sensitivity to Inter-Symbol Interference (ISI) caused by the multipath propagation in the wireless communication, which degrades the BER performance. Other methods that avoid the usage of delay units are proposed in [26] and [27]. In [26], the reference signals and information bearing signals, generated by a logistic map passes through a square-root-raised-cosine (SRRC) filter, are separated by a sinusoidal and its orthogonal signals (referred to as PS-DCSK for brief). This method also avoids the delay units and achieves twice as much data rate as the original DCSK. In [27], the DCSK system using a First Order Hybrid System and orthogonal sinusoidal carriers to separate the reference signal and information bearing signal in order to achieve doubled data transmission rate (referred to as FOHS-DCSK for brief). Moreover, a corresponding matched filter [28]–[30] is used to resist the channel distortion and multipath propagation, thus improving the BER performance. However, the chaotic baseband signal in the FOHS-DCSK generated by the basis function does not satisfy the Nyquists ISI-free criterion [31], which restricts the lower bound on the BER performance of the FOHS-DCSK.

A new DCSK scheme (SOHS-DCSK), using a second order hybrid system, is proposed in this work to reduce the ISI in order to achieve lower BER and to encode an additional bit stream transmission in the chaotic signal in order to achieve higher bit transmission rate as compared to FOHS-DCSK and PS-DCSK. The proposed SOHS-DCSK provides two sub-streams within a symbol duration according to the different reliability requirements, where the High Priority (HP) sub-stream could be used to transmit the important data information, at the same time, the Low Priority (LP) sub-stream could be used to transmit the lower importance information, such as voice information. At the transmitter, the LP bit stream is encoded into the chaotic signal generated by the convolution of the information bit and the basis function. The chaotic signal containing the LP information bits is used as the reference signal and the information bearing signal after multiplying with the HP information bit. Then, the reference signal and the information bearing signal are transmitted separated by orthogonal sinusoidal carriers rather than using the time delay. Due to the carriers being transmitted simultaneously in the same time slot, SOHS-DCSK not only achieves double HP bit transmission rate, but also avoids the difficulty with the implementation of delay units faced by the conventional DCSK, moreover, achieves the additional LP bit stream transmission. The frequency modulation operation makes the proposed method compatible with the conventional transducer and antenna. At the receiver, the demodulation process is performed without chaos synchronization and channel equalization. The matched filter uses the convolution of the received signal and the time reverse of the basis function to relieve the effect of multipath and ambient noise. Then, the points with the maximum SNR, sampled from the outputs of the matched filters corresponding to the reference and information bearing signals, respectively, are used to recover the LP information bits and correlation operation to further decrease the BER of the HP bit information. Then the LP information bits are recovered.

The paper is organized as follows: The system configuration of the proposed SOHS-DCSK is introduced in Section II. Simulation analysis of the proposed SOHS-DCSK and comparison with the conventional DCSK [13], NR-DCSK [18], HE-DCSK [20], RM-DCSK [21], I-DCSK [25], PS-DCSK [26] and FOHS-DCSK [27] are given in Section III. Experimental comparison results in different scenarios are given in Section IV. Finally, conclusions are given in Section V.

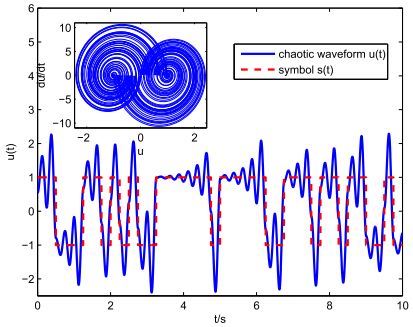

FIGURE 1. The time series of the continuous state $u(t)$ and discrete state $s(t)$ with $f = 4Hz$, the inset shows a phase plot of the chaotic attractor.

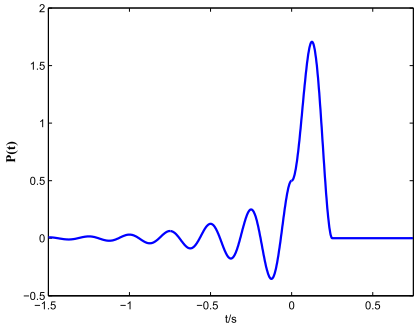

FIGURE 2. The basis function for the continuous state with the base frequency $f = 4Hz$.

II. SOHS-DCSK SYSTEM CONFIGURATION

A. SECOND ORDER HYBRID SYSTEM (SOHS)

The hybrid system contains a continuous state $u(t) \in R$ and a discrete symbol sequence $s(t) \in \{\pm 1\}$ given by [28]

$$\ddot{u}(t) - 2\beta\dot{u}(t) + \left(\omega^2 + \beta^2\right)(u(t) - s) = 0, \tag{1}$$

where ω and β are parameters satisfying $\omega = 2\pi f$, $\beta = f ln2$, and f is the base frequency of the chaotic signal. The discrete state s is defined by the guard condition

$$\dot{u}(t) = 0 \Rightarrow s(t) = sgn(u(t)), \tag{2}$$

where sgn is defined as

$$sgn(u) = \begin{cases} +1, & u \geq 0 \\ -1, & u < 0. \end{cases} \tag{3}$$

A typical time series of the continuous state $u(t)$ and discrete symbol sequence $s(t)$ are shown in Fig. 1, where the base frequency is $f = 4Hz$, the continuous state and discrete symbol are given with blue solid line and red dotted line, respectively. The inset shows a phase space projection of the chaotic attractor. Signal $u(t)$ in Eqs. (1)-(3) can be rewritten as a linear convolution using symbol sequence $s(t)$ and the basis function, given by

$$u(t) = \sum_{m=-\infty}^{\infty} s_m \cdot P(t - m), \tag{4}$$

where the basis function $P(t)$ is

$$P(t) = \begin{cases} \left(1 - e^{-\frac{\beta}{f}}\right) e^{\beta t}\left(\cos(\omega t) - \dfrac{\beta}{\omega}\sin(\omega t)\right), & t < 0 \\ 1 - e^{\beta\left(t - \frac{1}{f}\right)}\left(\cos(\omega t) - \dfrac{\beta}{\omega}\sin(\omega t)\right), & 0 \leq t < \dfrac{1}{f} \\ 0, & t \geq \dfrac{1}{f}. \end{cases} \tag{5}$$

Equations (4) and (5) act as a chaotic shape forming filter in digital communication as defined in [32], which together with the corresponding matched filter defined in the following Eq. (6) play a role of maximizing the signal to noise ratio [12]. The plot of the basis function with $f = 4Hz$ is shown in Fig. 2.

B. THE MATCHED FILTER CORRESPONDING TO THE HYBRID SYSTEM

At the receiver, a matched filter is given by

$$x(t) = \int_{-\infty}^{+\infty} v(\tau)\, g(t - \tau) d\tau, \tag{6}$$

where $v(t)$ is the filter input signal, $x(t)$ is the filter output signal, and $g(t) = P(-t)$ is the time reverse of the basis function. Equation (6) helps to relieve the effect of interference caused by multipath propagation and ambient noise, thus maximizing the SNR at the receiver.

C. THE PROPOSED SOHS-DCSK SCHEME

The block diagram of the proposed SOHS-DCSK is shown in Fig. 3. In the proposed method, the HP data transmission rate is R_b bits per second, corresponding to HP bit duration, T_b. The LP data transmission rate is R_s bits per second, corresponding to LP bit duration, T_s. The LP information bits are encoded into the chaotic signal using Eq. (4), which can be implemented by using simple electronic circuit in [4] or digital Finite Impulse Response (FIR) filter in [32]. The chaotic signal containing the LP information bits is used as the reference signal of the HP bit in the proposed SOHS-DCSK. The reference signal and the information bearing signal, obtained by the reference signal multiplied by the HP information bit, are separated by orthogonal sinusoidal carriers, which are generated by a numerically controlled oscillator (NCO). The transmitted signal for the HP information bit b_k^{HP} is given by

$$S_k(t) = u(t)\, sin(2\pi f_c t) + b_k^{HP} u(t)\, cos(2\pi f_c t), \quad (k-1)\Delta tL \leq t < k\Delta tL, \quad k = 1, 2, \ldots, n \tag{7}$$

where $u(t)$ is the chaotic signal containing the LP information bits, Δt is the sampling interval, f_c is the carrier frequency, n_{samp} is the number of sampling points for each LP bit duration T_s, N_s is the number of LP bits in one HP bit duration, defined as the spreading symbols, i.e., $N_s = T_b/T_s$, and $L = N_s * n_{samp}$ is the number of sampling points for each HP bit duration, which is referred to as spreading gain

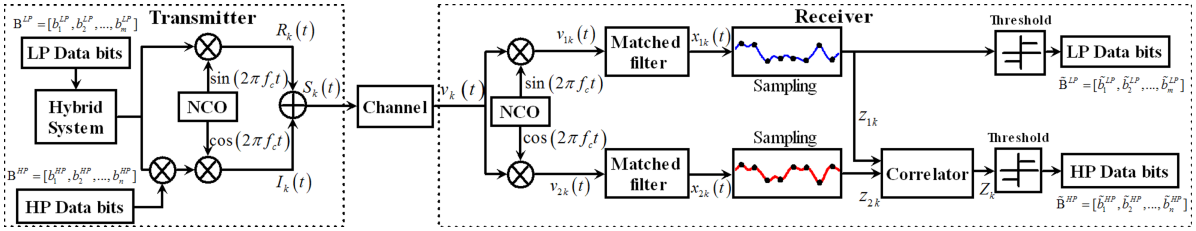

FIGURE 3. The block diagram of the proposed SOHS-DCSK.

in conventional DCSK system. Then, the HP bit duration is $T_b = \Delta t \cdot L$.

To illustrate the proposed method, we use the following example. Assume that two HP bits to be transmitted are $B_2^{HP} = [+1, -1]$ and the HP data transmission rate is $R_b = 1$ bit/s, as shown in Fig. 4(a) with blue solid line, where the HP bit duration $T_b = 1$s. Set the spreading symbols $N_s = 4$, $n_{samp} = 64$, carrier frequency $f_c = 10kHz$ and the base frequency of the chaotic signal $f = 4Hz$, then $T_s = 0.25s$ and $L = 256$, i.e., the LP bits data transmission rate is $R_s = 4$ bits/s. Assume that eight LP bits to be transmitted are $B_8^{LP} = \left[b_1^{LP}, b_2^{LP}, b_3^{LP}, b_4^{LP}, b_5^{LP}, b_6^{LP}, b_7^{LP}, b_8^{LP}\right] = [+1, +1, -1, -1, -1, -1, +1, -1]$, as shown in Fig. 4(a) with red dashed line. The eight LP bits information are encoded into the chaotic signal according to Eq. (4), where the symbol sequences $s(t)$ in Eq. (4) are replaced by the LP bits sequence B_8^{LP}, as shown in Fig. 4(b). The continuous state $u(t)$ (reference signal of HP bits) and LP bits information B_8^{LP} are given by the blue solid line and the red dotted line, respectively. It can be seen that four LP information bits encoded in one HP bit. The ISI of the second order hybrid system in Eq. (1) is much less than the ISI of the first order hybrid system in [27], which can be seen from the normalized auto-correlation of the basis function for the FOHS and SOHS, as given by the red dotted line and the blue solid line, respectively, in Fig. 4(c). Then, the frequency spectrum of the chaotic signal is shifted by the frequency modulation in Eq. (7) to the spectrum centered by the carrier frequency, as shown in Fig. 4(d), which makes the proposed method compatible with the conventional transducer and antenna. After the transmitted signal passes through the communication channel, the received signal is shown by the black solid line in Fig. 4(e), and the transmitted signal is also plotted using blue dashed line in the same figure for comparison purpose. At the receiver, the received signal $v_k(t)$ is firstly multiplied by the synchronized orthogonal carriers, respectively, to obtain the demodulation signal $v_{1k}(t)$ and $v_{2k}(t)$ given by

$$\begin{aligned} v_{1k}(t) &= v_k(t)\sin\left(2\pi\left(f_c+\Delta f\right)t\right) \\ &= \left(S_k(t) * h(t)\right)\sin\left(2\pi\left(f_c+\Delta f\right)t\right), \\ v_{2k}(t) &= v_k(t)\cos\left(2\pi\left(f_c+\Delta f\right)t\right) \\ &= \left(S_k(t) * h(t)\right)\cos\left(2\pi\left(f_c+\Delta f\right)_c t\right), \\ \Delta t(k-1)L &\le t < \Delta tkL, \end{aligned} \tag{8}$$

where $h(t)$ is the impulse response of the channel, Δf is frequency offset caused by the channel and the communication equipment, and $''*''$ denotes as the convolution operation. Given that demodulated signals are fed into the matched filter in Eq. (6), the matched filters output signals, $x_{1k}(t)$ and $x_{2k}(t)$, are shown using the blue dashed line and red solid line, respectively, in Fig. 4(f). The interference is reduced significantly in the filter output signals. The optimal SNR point sequences z_{1k} and z_{2k} for information bit, b_k, are obtained by sampling the matched filter output signals, $x_{1k}(t)$ and $x_{2k}(t)$, with a fixed interval, T_b/N_s, respectively, which are given by

$$\begin{aligned} z_{1k}(i) &= x_{1k}\left((k-1)T_b + \frac{T_b}{N_s}(i-1) + \frac{n_{samp}}{2}\Delta t\right) \\ z_{2k}(i) &= x_{2k}\left((k-1)T_b + \frac{T_b}{N_s}(i-1) + \frac{n_{samp}}{2}\Delta t\right), \end{aligned} \tag{9}$$

where $1 \le i \le N_s$, $z_{1k}(i)$ and $z_{2k}(i)$ are marked using pentagrams on the waveform of $x_1(t)$ and $x_2(t)$, respectively, in Fig. 4(f). The optimal SNR point sequence $z_{1k}(i)$ is used to recover the LP information bits, as given by

$$\tilde{b}^{LP}_{(k-1)\cdot N_s+i} = \begin{cases} +1, & z_{1k}(i) > 0 \\ -1, & z_{1k}(i) \le 0, \end{cases} \tag{10}$$

and the sequences $z_{1k}(i)$ and $z_{2k}(i)$ are also used for correlation detection in order to recover the kth HP information bit

$$Z_k = \sum_{i=1}^{N_s} z_{1k}(i)\, z_{2k}(i), \tag{11}$$

and the kth HP information bit is recovered as

$$\tilde{b}_k^{HP} = \begin{cases} +1, & Z_k > 0 \\ -1, & Z_k \le 0. \end{cases} \tag{12}$$

III. PERFORMANCE ANALYSIS

A. AWGN CHANNEL

In order to analyze the BER performance of the proposed method, the process of the channel modulation is ignored for simplicity. The received reference signal and the information bearing signal are given, respectively, by

$$\begin{aligned} v_{1k}(t) &= u(t) + w_1(t) \\ v_{2k}(t) &= b_k^{HP} u(t) + w_2(t), \end{aligned} \tag{13}$$

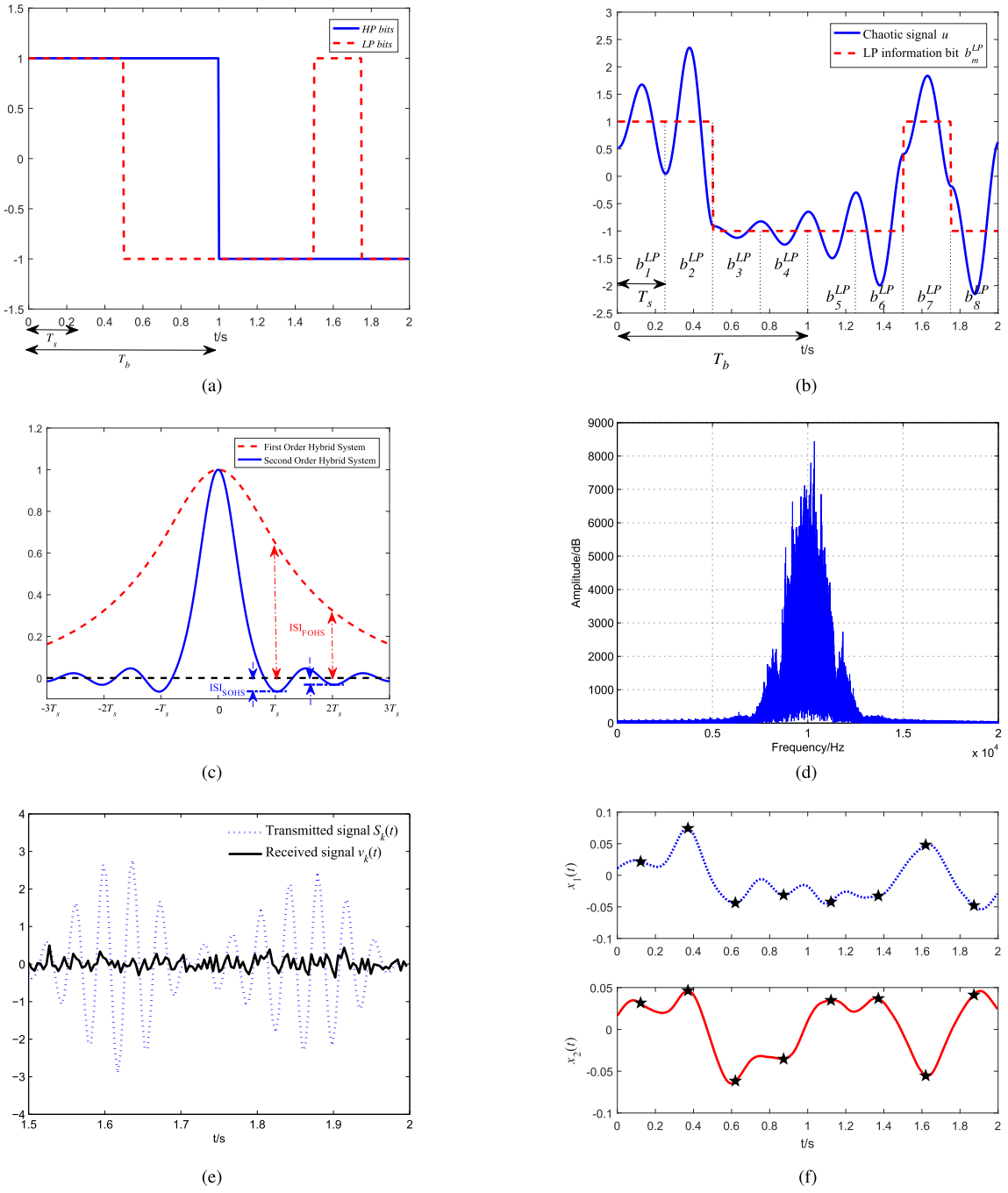

FIGURE 4. The schematic illustration of the proposed SOHS-DCSK. (a) The bits to be transmitted. (b) The chaotic signal generated by the hybrid system. (c) The auto-correlation of the basis function in the first order hybrid system and in the second order hybrid system. (d) The frequency spectrum of the transmitted signal. (e) The received signal after passing through the communication channel. (f) The filter output signal and the sampled points with optimal SNR marked by pentagrams in the corresponding filter outputs.

where $w_1(t)$ and $w_2(t)$ are the Gaussian white noise in the reference signal and the information bearing signal, respectively. The outputs of the matched filters for the kth information bit are

$$x_{1k}(t) = \sum_{m=-\infty}^{\infty} s_{1,m} \int_{-\infty}^{\infty} P(\tau) P\left(\tau - t + \frac{m}{f}\right) d\tau + \int_{-\infty}^{\infty} w_1(\tau) P(\tau - t) d\tau$$

$$x_{2k}(t) = b_k^{HP} \sum_{m=-\infty}^{\infty} s_{2,m} \int_{-\infty}^{\infty} P(\tau) P\left(\tau - t + \frac{m}{f}\right) d\tau + \int_{-\infty}^{\infty} w_2(\tau) P(\tau - t) d\tau, \quad (14)$$

where m is the mth symbol during kth HP information bit. The filters outputs are sampled at $t = n/f$ to get the following sampled data

$$\begin{aligned} z_{1k}(n) &= s_n I_n + \xi_{1k} + N_1 \\ z_{2k}(n) &= b_k^{HP} s_n I_n + \xi_{2k} + N_2, \end{aligned} \tag{15}$$

where f is the base frequency of the chaotic signal, $1 \le n \le N_s$ means the nth chaotic symbol in the kth HP bit duration T_b. I_n is the autocorrelation of the basis function $P(t)$ at $m = n$, given by

$$I_n = 1 + \left(1 - e^{-\beta}\right) \frac{\omega^2 - 3\beta^2}{2\beta\left(\omega^2 + \beta^2\right)}, \tag{16}$$

ξ_{ik} $(i = 1, 2)$ are the inter-symbol interferences (ISI) caused by the reference chaotic signal and the information bearing chaotic signal, respectively, given by

$$\xi_{ik} = \sum_{\substack{m=-\infty \\ m \ne n}}^{\infty} s_{i,m} \int_{-\infty}^{\infty} P(\tau) P\left(\tau - t + \frac{m}{f}\right) d\tau, \tag{17}$$

and $N_i = \int_{-\infty}^{\infty} w_i(\tau) P(\tau) d\tau$, $(i = 1, 2)$ are the filtered noise with zero mean and the variance equal to $\frac{N_0}{2} I_n$, according to the analysis in [12] and [33]. The decision variable for the kth HP bit b_k^{HP} is given by

$$\begin{aligned} Z_k &= \sum_{n=1}^{N_s} z_{1k}(n) z_{2k}(n) \\ &= \sum_{n=1}^{N_s} \left(s_n I_n + \xi_{1k} + N_1\right)\left(b_k^{HP} s_n I_n + \xi_{2k} + N_2\right) \\ &= \sum_{n=1}^{N_s} \left(b_k^{HP} s_n^2 I_n^2 + s_n I_n S_{2k} + b_k^{HP} s_n I_n S_{1k} + S_{1k} S_{2k}\right), \end{aligned} \tag{18}$$

where $S_{ik} = \xi_{ik} + N_i$ $(i = 1, 2)$, and the density function of ξ_{ik} is

$$f(\xi_{ik}) = \begin{cases} \dfrac{1}{I_n - 1} - \dfrac{|\xi_{ik}|}{(I_n - 1)^2}, & |\xi_{ik}| \le I_n - 1 \\ 0, & otherwise, \end{cases} \tag{19}$$

as given by [34]. Expectation of the decision variable Z_k is obtained by

$$\begin{aligned} &E(Z_k) \\ &= E\left(\sum_{n=1}^{N_s} b_k^{HP} s_n^2 I_n^2 + s_n I_n S_{2k} + b_k^{HP} s_n I_n S_{1k} + S_{1k} S_{2k}\right) \\ &= b_k^{HP} N_s I_n^2 E\left(s_n^2\right) + I_n E(s_n) E(S_{2k}) \\ &\quad + b_k^{HP} I_n^2 E(s_n) E(S_{1k}) + 2\int_{-(I_n-1)}^{I_n-1} \xi_{1k} f(\xi_{1k}) d\xi_{1k}, \end{aligned} \tag{20}$$

where $E(\cdot)$ represents the expectation operator and N_s is the number of spreading symbol in one bit. Because $E(s_n) = 0$ based on the statistical characteristics of the transmitted chaotic signal and $\int_{-(I_n-1)}^{I_n-1} \xi_{1k} f(\xi_{1k}) d\xi_{1k} = 0$, the expectation of Z_k is given by

$$E(Z_k) = b_k^{HP} N_s I_n^2 E\left(s_n^2\right). \tag{21}$$

The energy required to transmit one HP bit would be $E_b^{HP} = 2N_s E\left(s_n^2\right)$, then

$$E(Z_k) = b_k^{HP} \frac{E_b^{HP}}{2} I_n^2. \tag{22}$$

Subsequently, the variance of Z_k is

$$\begin{aligned} &D(Z_k) \\ &= N_s I_n^4 D\left(s_n^2\right) + N_s I_n^2 D(s_n) D(S_{2k}) \\ &\quad + N_s I_n^2 D(s_n) D(S_{1k}) + N_s D(S_{1k} S_{2k}) \\ &= 2N_s I_n^2 \frac{E_b^{HP}}{2N_s}\left(\frac{N_0}{2} I_n + \int_{-(I_n-1)}^{I_n-1} (\xi_{2k} - E(\xi_{2k}))^2 f(\xi_{2k}) d\xi_{2k}\right) \\ &\quad + N_s\left(\left(\int_{-(I_n-1)}^{I_n-1} (\xi_{1k} - E(\xi_{1k}))^2 f(\xi_{1k}) d\xi_{1k}\right)^2\right. \\ &\quad \left. + 2N_0 I_n \int_{-(I_n-1)}^{I_n-1} (\xi_{1k} - E(\xi_{1k}))^2 f(\xi_{1k}) d\xi_{1k} + \frac{N_0^2}{4} I_n^2\right) \\ &= \frac{E_b^{HP}}{2} I_n^3 N_0 + \frac{1}{6} E_b^{HP} I_n^2 (I_n - 1)^2 + \frac{1}{2} N_0^2 I_n^2 N_s \\ &\quad + \frac{1}{6} N_s N_0 I_n (I_n - 1)^2 + \frac{1}{36} N_s (I_n - 1)^4, \end{aligned} \tag{23}$$

where $D(\cdot)$ represents the variance operator. As a result, the analytical BER expression of high priority for the SOHS-DCSK can be given as

$$\begin{aligned} &P_{AWGN}^{HP} \\ &= \frac{1}{2} erfc\left(\left(\frac{4}{I_n}\frac{N_0}{E_b^{HP}} + \frac{4(I_n - 1)^2}{3I_n^2 E_b^{HP}} + \frac{4N_s}{I_n^2}\left(\frac{N_0}{E_b^{HP}}\right)^2\right.\right. \\ &\quad \left.\left. + \frac{4N_s(I_n - 1)^2}{3I_n^3 E_b^{HP}}\frac{N_0}{E_b^{HP}} + \frac{2N_s(I_n - 1)^4}{9I_n^4 \left(E_b^{HP}\right)^2}\right)^{-\frac{1}{2}}\right), \end{aligned} \tag{24}$$

where $erfc(\cdot)$ is the complementary error function. In addition, the LP bit energy is equal to $E_b^{LP} = \frac{1}{2N_s} E_b^{HP}$. According to the results in [34], the analytical BER expression of LP bit for the SOHS-DCSK can be given as

$$\begin{aligned} &P_{AWGN}^{LP} \\ &= \frac{1}{4(I_n - 1)^2}\left\{\left[(2I_n - 1)^2 + {G_1}^2\right] erfc\left(\frac{(2I_n - 1)}{G_1\sqrt{2}}\right)\right. \\ &\quad \left. -2\left(I_n^2 + {G_1}^2\right) erfc\left(\frac{I_n}{G_1\sqrt{2}}\right) + \left(1 + {G_1}^2\right) erfc\left(\frac{1}{G_1\sqrt{2}}\right)\right\} \\ &\quad - \frac{G_1}{4(I_n - 1)^2}\sqrt{\frac{2}{\pi}}\left\{(2I_n - 1)\exp\left(-\frac{(2I_n - 1)^2}{2{G_1}^2}\right)\right. \\ &\quad \left. - 2I_n \exp\left(-\frac{I_n^2}{2{G_1}^2}\right) + \exp\left(-\frac{1}{2{G_1}^2}\right)\right\}, \end{aligned} \tag{25}$$

where $G_1 = \sqrt{N_s I_n^2 \frac{N_0}{E_b^{HP}}}$.

B. WIRELESS CHANNEL

The transmitted signal passes through a wireless channel given by

$$h(t) = \sum_{l=0}^{L-1} \alpha_l \delta(t - \tau_l), \tag{26}$$

where L is the number of multipaths, α_l and τ_l are the attenuation and time delay corresponding to path l, and $\delta(\cdot)$ is the Dirac δ function. The received signals of reference and information bearing signals are

$$\begin{aligned} v_{1k}(t) &= h(t) * u(t) + w_1(t) \\ &= \sum_{l=0}^{L-1} \alpha_l u(t - \tau_l) + w_1(t) \\ &= \sum_{l=0}^{L-1} \alpha_l \sum_{m=-\infty}^{\infty} s_{1,m} P(t - \tau_l - m/f) + w_1(t), \end{aligned} \tag{27}$$

and

$$\begin{aligned} &v_{2k}(t) \\ &= h(t) * b_k^{HP} u(t) + w_2(t) \\ &= \sum_{l=0}^{L-1} \alpha_l b_k^{HP} u(t - \tau_l) + w_2(t) \\ &= \sum_{l=0}^{L-1} \alpha_l \sum_{m=-\infty}^{\infty} b_k^{HP} s_{2,m} P\left(t - \tau_l - \frac{m}{f}\right) + w_2(t), \end{aligned} \tag{28}$$

where '*' denote as convolution operation; the other notations are the same as Section III-A. The outputs of the matched filter for kth information bit are

$$\begin{aligned} x_{1k}(t) &= g(t) * v_{1k}(t) = \int_{\tau=-\infty}^{\infty} P(-\tau) v_{1k}(t - \tau) d\tau \\ &= \sum_{l=0}^{L-1} \alpha_l \sum_{m=-\infty}^{\infty} s_{1,m} \left(\int_{\tau=-\infty}^{\infty} P(\tau) P\left(\begin{matrix} \tau - t \\ +\tau_l + \frac{m}{f} \end{matrix} \right) d\tau \right) \\ &\quad + \int_{\tau=-\infty}^{\infty} w_1(\tau) P(\tau - t) d\tau, \end{aligned} \tag{29}$$

and

$$\begin{aligned} &x_{2k}(t) \\ &= g(t) * v_{2k}(t) \\ &= b_k^{HP} \sum_{l=0}^{L-1} \alpha_l \sum_{m=-\infty}^{\infty} s_{2,m} \left(\int_{\tau=-\infty}^{\infty} P(\tau) P\left(\begin{matrix} \tau - t + \\ \tau_l + \frac{m}{f} \end{matrix} \right) d\tau \right) \\ &\quad + \int_{\tau=-\infty}^{\infty} P(\tau - t) w_2(\tau) d\tau. \end{aligned} \tag{30}$$

According to [12], two filters outputs are sampled at $t = n/f$, we have

$$\begin{aligned} &z_{1k}(n) \\ &= \sum_{l=0}^{L-1} \alpha_l \sum_{m=-\infty}^{\infty} s_{1,m} \left(\int_{\tau=-\infty}^{\infty} P(\tau) P\left(\begin{matrix} \tau - t + \tau_l \\ + \frac{m-n}{f} \end{matrix} \right) d\tau \right) \\ &\quad \times \int_{\tau=-\infty}^{\infty} w_1(\tau) P(\tau - t) d\tau \\ &= \sum_{l=0}^{L-1} \sum_{m=-\infty}^{\infty} s_{1,m} C_{l,m-n} + N_1 \\ &= \sum_{l=0}^{L-1} s_n C_{l,0} + \sum_{l=0}^{L-1} \sum_{\substack{m=-\infty \\ m \neq n}}^{\infty} s_{1,m} C_{l,m-n} + N_1 \\ &= s_n \Theta + \Xi_{1k} + N_1, \end{aligned} \tag{31}$$

and

$$\begin{aligned} z_{2k}(n) &= b_k^{HP} \sum_{l=0}^{L-1} \sum_{m=-\infty}^{\infty} s_{2,m} C_{l,m-n} + N_2 \\ &= b_k^{HP} \sum_{l=0}^{L-1} s_n C_{l,0} + \sum_{l=0}^{L-1} \sum_{\substack{m=-\infty \\ m \neq n}}^{\infty} s_{2,m} C_{l,m-n} + N_2 \\ &= b_k^{HP} s_n \Theta + \Xi_{2k} + N_2, \end{aligned} \tag{32}$$

where $\Theta = \sum_{l=0}^{L} C_{l,0}$ is the sum of the multipath power for the nth chaotic symbol s_n. The ISI of LP bit caused by multipath propagation is

$$\begin{aligned} \Xi_{ik} &= \sum_{l=0}^{L-1} \sum_{\substack{m=-\infty \\ m \neq n}}^{\infty} s_{i,m} C_{l,m-n} \\ &= \underbrace{\sum_{l=0}^{L-1} \sum_{m=-\infty}^{n-1} s_{i,m} C_{l,m-n}}_{I_{past}} + \underbrace{\sum_{l=0}^{L-1} \sum_{m=n+1}^{\infty} s_{i,m} C_{l,m-n}}_{I_{future}}, \end{aligned}$$

where I_{past} and I_{future} are the ISI from past symbols and future symbols, respectively.

$$C_{l,m-n} = \alpha_l \int_{\tau=-\infty}^{\infty} P(\tau) P\left(\tau + \tau_l + \frac{m-n}{f}\right) d\tau$$

is obtained by

$$\begin{aligned} &C_{l,m-n} \\ &= \begin{cases} \alpha_l D \left(2 - e^{-\frac{\beta}{f}} - e^{\frac{\beta}{f}}\right) (A \cos(\omega\tau_l) + B \sin(\omega\tau_l)), \\ \qquad\qquad \left|\tau_l + \frac{m-n}{f}\right| \geq \frac{1}{f} \\ \alpha_l \begin{bmatrix} A\left(D\left(2 - e^{-\frac{\beta}{f}}\right) - D^{-1} e^{-\frac{\beta}{f}}\right) \cos(\omega\tau_l) \\ +B\left(D\left(2 - e^{-\frac{\beta}{f}}\right) + D^{-1} e^{-\frac{\beta}{f}}\right) \sin(\omega\tau_l) \\ +1 - |\tau_l f| + m - n \end{bmatrix}, \\ \qquad\qquad 0 \leq \left|\tau_l + \frac{m-n}{f}\right| < \frac{1}{f} \end{cases} \end{aligned} \tag{33}$$

where $A = \frac{(\omega^2 - 3\beta^2)f}{4\beta(\omega^2 + \beta^2)}$, $B = \frac{(3\omega^2 - \beta^2)f}{4\omega(\omega^2 + \beta^2)}$, and $D = e^{-\beta\left|\tau_l + \frac{m-n}{f}\right|}$. The decision variable Z_k for kth HP information bit b_k^{HP} can

be given as

$$\begin{aligned} Z_k &= \sum_{n=1}^{N_s} z_{1k}(n)\, z_{2k}(n) \\ &= \sum_{n=1}^{N_s} (s_n\Theta + \Xi_{1k} + N_1)\left(b_k^{HP} s_n\Theta + \Xi_{2k} + N_2\right) \\ &= \sum_{n=1}^{N_s} \left(b_k^{HP} s_n^2\Theta^2 + s_n\Theta H_{2k} + b_k^{HP} s_n\Theta H_{1k} + H_{1k}H_{2k}\right), \end{aligned} \tag{34}$$

where $H_{ik} = \Xi_{ik} + N_i$ $(i = 1, 2)$, $\Xi_{ik} = I_{past} + I_{future}$, and I_{past} and I_{future} are uniform distribution

$$I_{past} = I_{future} \sim U\left(-\left|\frac{K}{e^{\frac{\beta}{f}} - 1}\right|, \left|\frac{K}{e^{\frac{\beta}{f}} - 1}\right|\right), \tag{35}$$

where

$$K = \sum_{l=0}^{L} \alpha_l \left(2 - e^{-\frac{\beta}{f}} - e^{\frac{\beta}{f}}\right) e^{-\beta\tau_l} \left(A\cos(\omega\tau_l) + B\sin(\omega\tau_l)\right)$$

according to [12]. Therefore, the expectation of the decision variable Z_k is

$$E(Z_k) = \frac{1}{2} E_b^{HP} \Theta^2, \tag{36}$$

and the variance of Z_k is

$$\begin{aligned} &D(Z_k) \\ &= N_s D\left(s_n^2\right)\Theta^4 + 2N_s D(s_n)\Theta^2 D(H_{1k}) + N_s D(H_{1k}) D(H_{2k}) \\ &= \Theta^2 E_b^{HP}\left(\frac{2}{3}\left(\frac{K}{e^{\beta}-1}\right)^2 + \frac{N_0}{2}\Theta\right) + N_s\left(\frac{2}{3}\left(\frac{K}{e^{\beta}-1}\right)^2 + \frac{N_0}{2}\Theta\right)^2 \\ &= \frac{2}{3}\Theta^2 E_b^{HP}\left(\frac{K}{e^{\beta}-1}\right)^2 + \frac{N_0}{2} E_b^{HP}\Theta^3 + N_s\left(\frac{2}{3}\left(\frac{K}{e^{\beta}-1}\right)^2\right)^2 \\ &\quad + N_s\frac{N_0^2}{4}\Theta^2 + \frac{2}{3}N_s N_0\Theta\left(\frac{K}{e^{\beta}-1}\right)^2. \end{aligned} \tag{37}$$

Finally, the BER for HP information bits over the wireless channel is

$$P_{Multipath}^{HP} = \frac{1}{2} erfc\left(\frac{E(Z_k)}{\sqrt{2D(Z_k)}}\right), \tag{38}$$

where

$$\begin{aligned} &\frac{E(Z_k)}{\sqrt{2D(Z_k)}} \\ &= \left(\begin{array}{c} \frac{16}{3E_b^{HP}\Theta^2}\left(\frac{K}{e^{\beta}-1}\right)^2 + \frac{4}{\Theta}\frac{N_0}{E_b^{HP}} + \\ \frac{8N_s}{\Theta^4}\left(\frac{2}{3}\left(\frac{K}{e^{\beta}-1}\right)^2\right)^2 + \frac{2N_s}{\Theta^2}\left(\frac{N_0}{E_b^{HP}}\right)^2 \\ + \frac{16N_s}{3E_b^{HP}\Theta^3}\left(\frac{K}{e^{\beta}-1}\right)^2\frac{N_0}{E_b^{HP}} \end{array}\right)^{-\frac{1}{2}}, \end{aligned}$$

and $erfc(\cdot)$ is the complementary error function, defined as

$$erfc(x) = \frac{2}{\sqrt{\pi}}\int_x^{\infty} e^{-t^2} dt \tag{39}$$

According to [12], the BER expression of LP information bit can be given as

$$\begin{aligned} &P_{Multipath}^{LP} \\ &= \sqrt{2G_2^2}\frac{e^{\frac{\beta}{f}} - 1}{4|K|}\left\{\begin{array}{l} z_1 \cdot erfc(z_1) - z_2 \cdot erfc(z_2) \\ -e^{-z_1^2}/\sqrt{\pi} + e^{-z_2^2}/\sqrt{\pi} \end{array}\right\}, \end{aligned} \tag{40}$$

where $z_1 = \frac{\Theta + \frac{|K|}{e^{\beta/f}-1}}{\sqrt{2G_2^2}}$, $z_2 = \frac{\Theta - \frac{|K|}{e^{\beta/f}-1}}{\sqrt{2G_2^2}}$, and $G_2 = \sqrt{N_s\Theta^2\frac{N_0}{E_b^{HP}}}$.

In the next two Sections, simulation and experiment are conducted to test the performance of the proposed method.

IV. PERFORMANCE ANALYSIS OF THE PROPOSED METHOD BY SIMULATION

In order to validate the SOHS-DCSK method and compare it with the conventional DCSK [13], NR-DCSK [18], HE-DCSK [20], RM-DCSK [21], I-DCSK [25], PS-DCSK [26] and FOHS-DCSK [27], the simulation results over the additive white Gaussian noise (AWNG) channel and wireless channel are given in this Section.

A. PERFORMANCE SIMULATION IN THE AWGN CHANNEL

Figure 5 shows BER performance results for the proposed SOHS-DCSK, the conventional DCSK [13], NR-DCSK [18], HE-DCSK [20], RM-DCSK [21], I-DCSK [25], PS-DCSK [26] and FOHS-DCSK [27] with the same number of sampling points $L = 512$, and the same data transmission rate $R_b = 187.5$ bits/s, where the sampling frequency $f_s = 96kHz$, $N_s = 8$, and $n_{samp} = 64$ for the proposed method. The carrier frequency is set as $f_c = 1.8kHz$ for SOHS-DCSK, FOHS-DCSK and PS-DCSK. The duplicated times $p = 8$ in the NR-DCSK, the bit transmission rate and system parameters are given in Table 1, where the $Eb/N0$ is 12dB. Figure 5 gives the BER comparisons of different methods for the same spreading gain in subplot (a) and for the same data transmission rate in subplot (b), respectively. We can see from Fig. 5(a) that the HE-DCSK and the RM-DCSK have similar BER, and slightly worse than the PS-DCSK, but outperform the DCSK. I-DCSK and NR-DCSK reduce the BER as compared to DCSK. The performance of FOHS-DCSK is degraded as compared to NR-DCSK and I-DCSK with the increasing SNR. This is because the basis function, which forms the chaotic signal in FOHS-DCSK, has large ISI; the ISI becomes dominant in the BER performance as the SNR level increasing. Figure 5(b) show the BER comparison with the same data transmission rate of 187.5 bits/s, we establish that BER of the HP information bits of the proposed method shows the best BER performance among the comparison methods over the AWGN channel and even the BER of the LP information bits outperforms comparison methods except NR-DCSK and FOHS-DCSK in Table 1. It should be noted

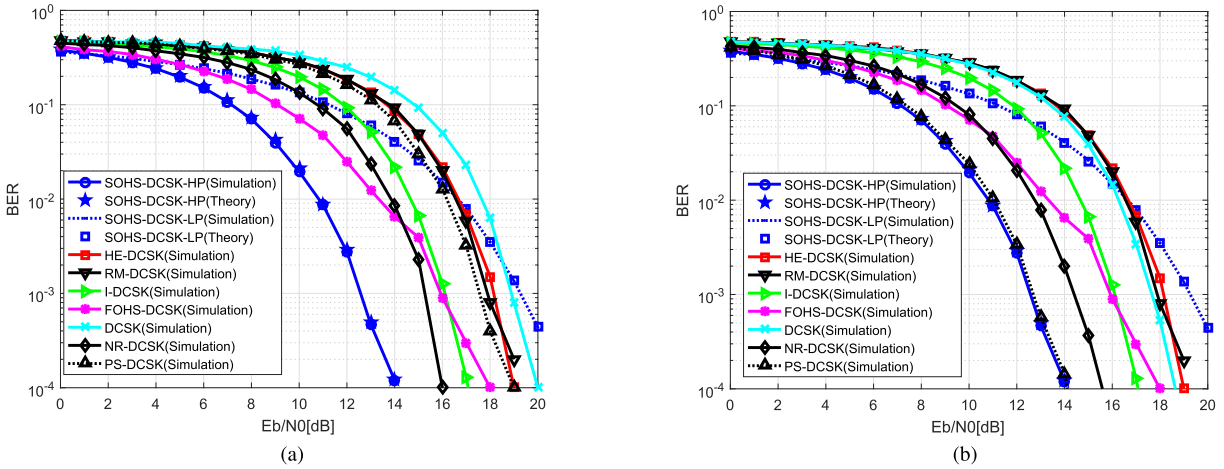

FIGURE 5. Simulation BER over AWGN channel for SOHS-DCSK, DCSK, HE-DCSK, RM-DCSK, I-DCSK, FOHS-DCSK, PS-DCSK and NR-DCSK. (a) BER comparison with the same spreading gain equal to $L = 512$ for AWGN channel. (b) BER comparison with the same transmission rate equal to 187.5 bits/s for AWGN channel.

TABLE 1. Performance comparison between the enhanced DCSK variants and the proposed method in the AWGN channel with the same number of sampling points $L = 512$.

	Chaotic signal	Bit transmission rate		BER	Spreading gain	Carrier parameters	
		HP	LP			Carrier frequency	Sampling frequency
DCSK	logistic map	93.75 bits/s	-	24.84%	512	-	$96kHz$
HE-DCSK	logistic map	187.5 bits/s	-	18.27%	512	-	
RM-DCSK	logistic map	187.5 bits/s	-	18.62%	512	-	
I-DCSK	logistic map	187.5 bits/s	-	9.39%	512	-	
NR-DCSK	logistic map	93.75 bits/s	-	5.57%	512(p=8)	-	
PS-DCSK	logistic map	187.5 bits/s	-	16.25% 0.31%	512(n_{samp}=1, N_s=512) 512(n_{samp}=64, N_s=8)	$1.8kHz$	
FOHS-DCSK	First order hybrid system	187.5 bits/s	-	2.48%	512 ($n_{samp} = 16$,$N_s = 32$)	$1.8kHz$	
SOHS-DCSK	Second order hybrid system	187.5 bits/s	1500 bits/s	0.23%(HP) 8.04%(LP)	512 ($n_{samp} = 64$, $N_s = 8$)	$1.8kHz$	

when $n_{samp} = 1$ is used in the PS-DCSK, that the BER performance is worse than the comparison methods, as shown in Fig. 5(a); when the same n_{samp} is used in the SOHS-DCSK and PS-DCSK, the SOHS-DCSK shows slightly better BER than the PS-DCSK, because SRRC is designed for the binary signal, as shown in Fig. 5(b). From Fig. 5, we gather that BERs for both the HP and the LP information bits of the SOHS-DCSK are close to the theoretical ones, and it is more robust to noise in the AWGN channel as compared with other DCSK variants. This is because the matched filter maximizes the SNR at the receiver, and the decision using multi-points with maximum SNR correlation further reduces the BER.

B. PERFORMANCE ANALYSIS IN THE WIRELESS CHANNEL

The BER performance of different methods in the wireless channel for the same spreading gain and the same bit transmission rate $R_b = 93.75$ bits/s are shown in Fig. 6(a) and Fig. 6(b), respectively, where $N_s = 16$ and $n_{samp} = 64$ for the proposed method. The average power gains of the first, second and third paths are $E_1 = 0.6$, $E_2 = 0.3$, and $E_3 = 0.1$ with delay $\tau_1 = 0$, $\tau_2 = 0.0042s$ and $\tau_3 = 0.0094s$, respectively. The sampling frequency of the Digital-to-Analog Converter (DAC) $f_s = 96kHz$, the system parameters configuration and performance comparison are given in Table 2, where the $Eb/N0$ is 12dB. As observed in Fig. 6, the I-DCSK performance degrades dramatically, it is even worse than the HE-DCSK and RM-DCSK, since I-DCSK is sensitive to ISI caused by multipath propagation. The enhancement of the performance in NR-DCSK is proportional to the duplicated times p. However, NR-DCSK is an Ultra Wide Band (UWB) communication method, which is not suitable for the complex bandwidth limited channel, such as the shortwave wireless channel and the underwater acoustic channel. The BER performance for HP information of the proposed SOHS-DCSK method is superior to other improved DCSK variants in the wireless channel.

TABLE 2. Performance comparison of the communication system parameters between the enhanced DCSK variants and the proposed method in the wireless channel with the same number of sampling points $L = 1024$.

	Chaotic signal	Bit transmission rate		BER	Spreading gain	Carrier parameters	
		HP	LP			Carrier frequency	Sampling frequency
DCSK	logistic map	46.875 bits/s	-	33.02%	1024	-	$96kHz$
HE-DCSK	logistic map	93.75 bits/s	-	29.09%	1024	-	
RM-DCSK	logistic map	93.75 bits/s	-	27.97%	1024	-	
I-DCSK	logistic map	93.75 bits/s	-	29.72%	1024	-	
NR-DCSK	logistic map	46.875 bits/s	-	13.41%	1024(p=8)	-	
PS-DCSK	logistic map	93.75 bits/s	-	38.17% 2.44%	1024(n_{samp}=1, N_s=1024) 1024(n_{samp}=64, N_s=16)	$1.8kHz$	
FOHS-DCSK	First order hybrid system	93.75 bits/s	-	5.32%	1024 ($n_{samp} = 16$,$N_s = 64$)	$1.8kHz$	
SOHS-DCSK	Second order hybrid system	93.75 bits/s	1500 bits/s	2.06%(HP) 20.52%(LP)	1024 ($n_{samp} = 64$, $N_s = 16$)	$1.8kHz$	

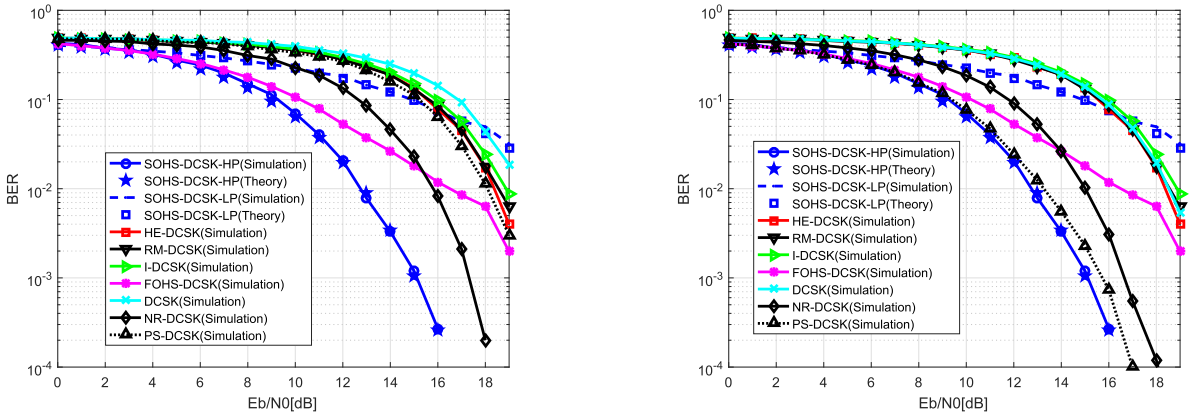

FIGURE 6. Simulation BER over wireless channel for SOHS-DCSK, DCSK, HE-DCSK, RM-DCSK, I-DCSK, FOHS-DCSK, PS-DCSK and NR-DCSK. (a) BER comparison with the spreading gain equal to $L = 1024$ for the wireless channel. (b) BER comparison with the transmission rate equal to 93.75 bits/s for the wireless channel.

The performance is greatly enhanced by using matched filter and multiple maximum SNR points correlation. As compared to FOHS-DCSK, the SOHS-DCSK achieves better performance due to the lower ISI caused by the chaotic signal in the proposed method. It should be noticed that the time-varying threshold in [12] is used to decode the LP information bits. The BER performances of HP and LP information bits over the wireless channel are consistent with the theoretical ones. In addition, at low $Eb/N0$ range, the BER performance of LP information stream is better than most comparison methods. The achieved BER comparison for AWGN channel, with the same data rate of 187.5 bits/s shown in Fig. 5(b) and the BER comparison for the wireless channel with the same data rate of 93.75 bits/s shown in Fig. 6(b), show that the proposed method has the best BER performance among the comparison methods for both the AWGN channel and the wireless channel. A point to be noticed here is that the shape forming filter and the corresponding matched filter are used, which achieves maximum signal to noise ratio. Therefore, the proposed method and the PS-DCSK, both using this configuration, outperform the conventional DCSK significantly. Both the shape forming filters, including the chaotic shape forming filter used by the proposed method and the square root raised cosine filter used in PS-DCSK, are designed for digital signal, namely [1,-1]. However, the logistic map output, i.e., a real number in [0, 1], being used in PS-DCSK as the shape forming filter input, slightly degrades the noise resistance performance of the corresponding matched filter. As a result, the performance of PS-DCSK is slightly inferior to the proposed method. If one keeps the spreading gain the same but $n_{samp} = 1$, as learned from PS-DCSK literature [26], the PS-DCSK degrades a lot as seen from Tables 1 and 2. However, the result of PS-DCSK is consistent with the result derived by using the same n_{samp} as that of our proposed method in this paper, which is also given in Tables 1 and 2.

Moreover, Figure 7 presents results on the influence of the parameter N_s versus BER performance under different

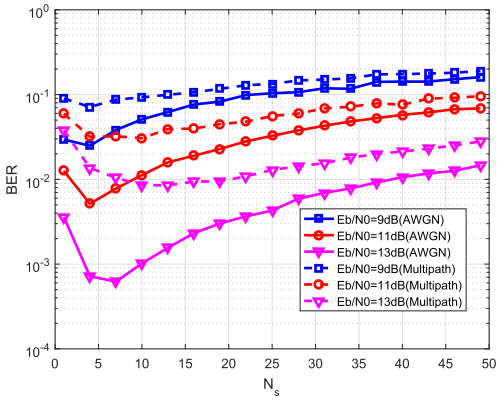

FIGURE 7. BER of the proposed method versus the parameter N_S over the AWGN channel and the wireless channel.

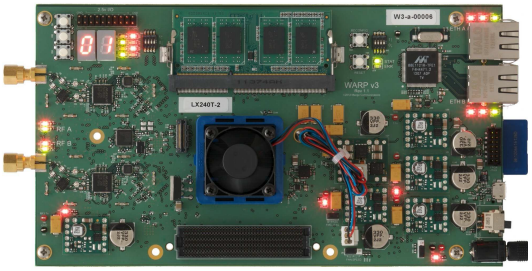

FIGURE 8. The photo of WARP.

SNRs of the proposed SOHS-DCSK over both the AWGN channel and the wireless channel, where the oversampling rate of each chaotic symbol duration is fixed as $n_{samp} = 64$, the number of the chaotic symbols, N_s, is increased from 1 to 50. The parameters of the wireless channel are as follow: The average power gains of the first and second paths are $[E_1, E_2] = [0.7, 0.3]$ with the delay vector $[\tau_1, \tau_2] = [0, 5.3]$ millisecond. We know that i) there is an optimal N_s (defined as N_{s_opt}) for a fixed E_b/N_0, when $N_s < N_{s\_opt}$, the BER is increasing with the decreasing of N_s; when $N_s > N_{s\_opt}$, the BER is increasing with the increasing of N_s. ii) The N_{s_opt} is increasing with the increasing of E_b/N_0. This is because the influence of ISI caused by the chaotic signal is dominant on BER with the increasing of E_b/N_0, while the cross-correlation of chaotic signal approaches 0 with the increasing of spreading gain. iii) N_{s_opt} is larger in the wireless channel as compared with the AWGN channel at the same E_b/N_0, because the larger N_s means optimal SNR sampling points to provide a better multi-path effect resistance.

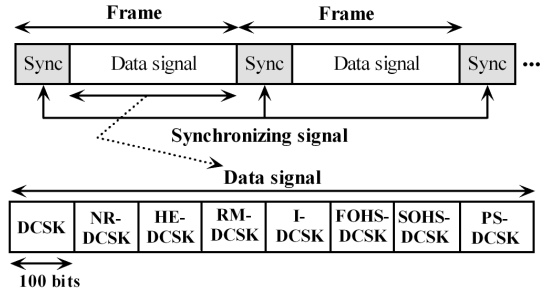

FIGURE 9. Frame structure used at the transmitter.

V. EXPERIMENT BASED ON WIRELESS OPEN-ACCESS RESEARCH PLATFORM (WARP)

The experimental implementation of the proposed SOHS-DCSK and the comparison methods are conducted using two Wireless Open-Access Research Platform (WARP) with Virtex-6 LX240T FPGA, as shown in Fig. 8. The sampling frequency of the Analog-to-Digital Converter (ADC) is $f_s = 40MHz$. At the transmitter, the information is grouped into frames, as shown in Fig. 9. The known Synchronizing (Sync) signals generated by logistic map are regularly inserted before valid data as a frame starter to implement the frame synchronization and frequency offset compensation

(a)

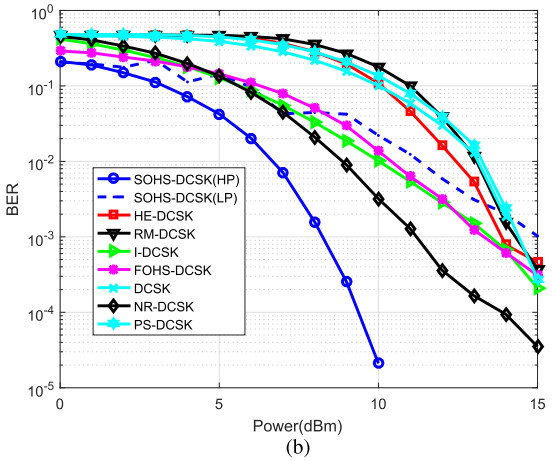

(b)

FIGURE 10. The first experimental scenario for comparison between the proposed SOHS-DCSK and the conventional DCSK, HE-DCSK, RM-DCSK, I-DCSK, FOHS-DCSK, NR-DCSK and PS-DCSK. (a) The test scenario photo. (b) The BER comparison in the first scenario for the different methods.

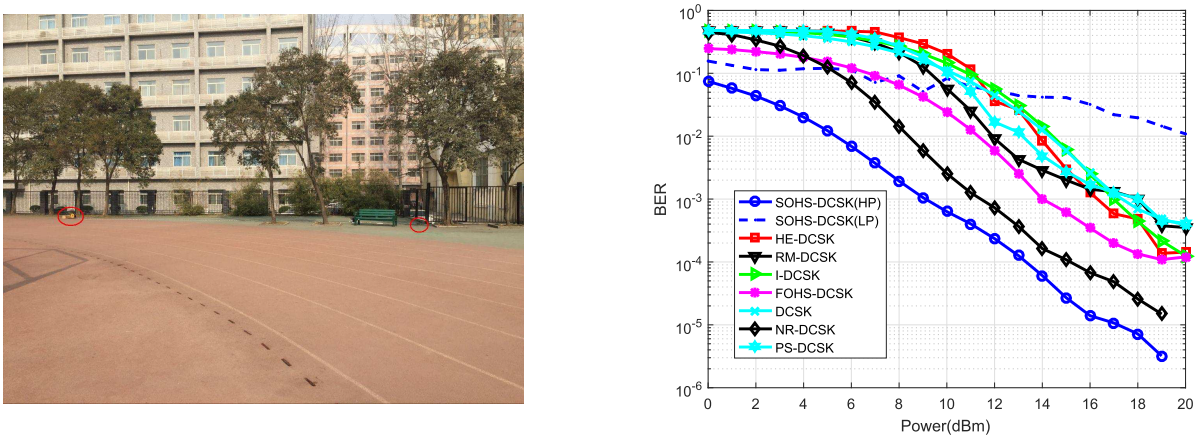

FIGURE 11. The second experimental for comparison between the proposed SOHS-DCSK and the conventional DCSK, HE-DCSK, RM-DCSK, I-DCSK, FOHS-DCSK, NR-DCSK and PS-DCSK. (a) The test scenario photo. (b) The BER comparison in the second scenario for the different methods.

at the receiver. The data in each frame includes the modulated signal pieces of 100 information bits for DCSK, NR-DCSK, HE-DCSK, RM-DCSK, I-DCSK, FOHS-DCSK, SOHS-DCSK, and PS-DCSK successively, making these methods to undergo the same channel distortion in order to ensure a fair test environment. In addition, the number of sampling points of these methods $L = 128$, wherein the $n_{samp} = 32$ in the SOHS-DCSK to achieve the optimal BER performance. $p = 8$ in the NR-DCSK. The carrier frequency is $f_c = 1MHz$ in the SOHS-DCSK, the FOHS-DCSK, and the PS-DCSK, then, the analog upcarrier of all comparison methods are implemented on the WARP transmitter.

The experimental results for two tests in different scenarios are given in Fig. 10 and Fig. 11, respectively. The corresponding channel parameter estimation results are given in the Appendix, which shows that the channel of the second test scenario is more complex than the first one. The locations of the transmitter and the receiver for the two test scenarios are marked by red circle in the Fig. 10(a) and Fig. 11(a), respectively. The horizontal axis of the Fig. 10(b) and Fig. 11(b) is the transmitter power, which is used to alter the SNR equivalently. In both Fig. 10 and Fig. 11, the oversampling of PS-DCSK is 1. From Fig. 10 and Fig. 11, we learn that the BER performances are consistent with the simulation results in practical wireless communication tests. We conclude that the proposed method is more robust to the interference caused by multipath propagation and ambient noise.

VI. CONCLUSIONS

In this work, a new DCSK method based on a second order hybrid system is proposed to get higher data transmission rate with respect to DCSK, and better BER performance as compared to the conventional DCSK and some of the enhanced DCSK variants. High data transmission rate is achieved by two-fold ways. The proposed SOHS-DCSK provides two sub-stream within a symbol, the LP sub-stream is encoded into the chaotic signal by convoluting with the basis function with the LP bits, which is used as the reference signal. The reference signal and the information bearing signal formed by multiplying the reference signal with HP sub-stream bit are separated by orthogonal sinusoidal carriers rather than the time delay unit in the conventional DCSK. It not only achieves double HP data transmission rate as compared to the conventional DCSK, but also achieves even higher information transmission rate for LP information. At the same time, it not only avoids the difficulty in transmitting broadband chaotic signals using the antenna or transducer with the limited bandwidth, but also avoids the difficulty in implementing time delay in the conventional DCSK. At the receiver, the proposed method performs demodulation without both chaos synchronization and channel equalization. The matched filter relieves the effect of multipath propagation and ambient noise, and the multiple maximum SNR correlation decision reduces the BER of HP information bit in the proposed method significantly. As compared to FOHS-DCSK in [27], the proposed method has much lower ISI caused by the basis function, thus achieving lower BER in both the AWGN channel and the wireless channel. Moreover, the frequency modulation in the SOHS-DCSK avoids the transmission of the wideband chaotic signal in the channel, which is compatible with the conventional communication equipment. The simulation and experimental results show the superiority of the SOHS-DCSK as compared to other enhanced DCSK variants, and better application potential in practical communication systems. The proposed scheme improves both the reliability and data transmission rate significantly of the communication system. A chaos property is used to enhance the conventional communication system performance without modification to the system hardware, which promises easy and brilliant application potential. In addition, the proposed method can be applied not only to short range UWB communication, such

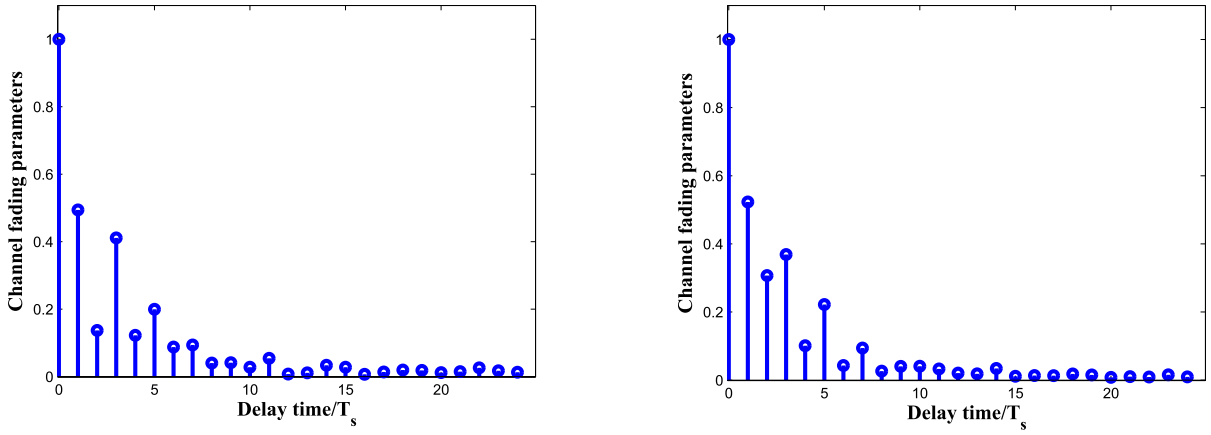

FIGURE 12. The channel parameter estimation for two experimental scenarios. (a) The estimated channel parameters of the first experimental scenario. (b) The estimated channel parameters of the second experimental scenario.

as Wi-Fi communication system protocol, but also to complex bandwidth limited channels, such as shortwave wireless channel and underwater acoustic channel.

APPENDIX

The channel parameters estimation results of the two experimental test scenarios are performed using the Least Squares (LS) algorithm, as shown in Fig. 12(a) and 12(b). The unit of delay time is defined as the symbol duration, i.e., $T_s = n_{samp}/f_s = 0.8\mu s$. It can be seen that the second test scenario channel is more complicated than the first one in the case of more paths involved.

REFERENCES

[1] S. T. Hayes, C. Grebogi, and E. Ott, "Communicating with chaos," *Phys. Rev. Lett.*, vol. 70, pp. 3031–3034, May 1993.

[2] S. Hayes, C. Grebogi, E. Ott, and A. Mark, "Experimental control of chaos for communication," *Phys. Rev. Lett.*, vol. 73, no. 13, pp. 1781–1784, Sep. 1994.

[3] H.-P. Ren, M. S. Baptista, and C. Grebogi, "Wireless communication with chaos," *Phys. Rev. Lett.*, vol. 110, no. 18, Apr. 2013, Art. no. 184101.

[4] H.-P. Ren, C. Bai, J. Liu, M. S. Baptista, and C. Grebogi, "Experimental validation of wireless communication with chaos," *Chaos, Interdiscipl. J. Nonlinear Sci.*, vol. 26, no. 8, p. 083117, Aug. 2016.

[5] G. Kaddoum, "Wireless chaos-based communication systems: A comprehensive survey," *IEEE Access*, vol. 4, pp. 2621–2648, May 2016.

[6] A. Argyris *et al.*, "Chaos-based communications at high bit rates using commercial fibre-optic links," *Nature*, vol. 438, pp. 343–346, Nov. 2005.

[7] C. E. Shannon, "Communication in the presence of noise," *Proc. IEEE*, vol. 86, no. 2, pp. 447–457, Feb. 1998.

[8] H.-P. Ren, C. Bai, K. Tian, and C. Grebogi, "Dynamics of delay induced composite multi-scroll attractor and its application in encryption," *Int. J. Non-Linear Mech.*, vol. 94, pp. 334–342, Sep. 2017.

[9] G. Kaddoum, F. Richardson, and F. Gagnon, "Design and analysis of a multi-carrier differential chaos shift keying communication system," *IEEE Trans. Commun.*, vol. 61, no. 8, pp. 3281–3291, Aug. 2013.

[10] H.-P. Ren, C. Bai, Q. Kong, M. S. Baptista, and C. Grebogi, "A chaotic spread spectrum system for underwater acoustic communication," *Phys. A, Stat. Mech. Appl.*, vol. 478, no. 15, pp. 77–92, Jul. 2017.

[11] J. Zhan, L. Wang, M. Katz, and G. R. Chen, "A differential chaotic bit-interleaved coded modulation system over multipath Rayleigh channels," *IEEE Trans. Commun.*, vol. 65, no. 12, pp. 5257–5265, Dec. 2017.

[12] J.-L. Yao, C. Li, H.-P. Ren, and C. Grebogi, "Chaos-based wireless communication resisting multipath effects," *Phys. Rev. E, Stat. Phys. Plasmas Fluids Relat. Interdiscip. Top.*, vol. 96, Sep. 2017, Art. no. 032226.

[13] G. Kolumbán, G. K. Vizvári, W. Schwarz, and A. Abel, "Differential chaos shift keying: A robust coding for chaos communication," in *Proc. 4th Int. Workshop Nonlinear Dyn. Electron. Syst.*, Seville, Spain, 1996, pp. 92–97.

[14] G. Kolumbán, G. Kis, M. P. Kennedy, and Z. Jákó, "FM-DCSK: A new and robust solution to chaos communications," in *Proc. Int. Symp. Non-Linear Theory Appl.*, 1997, pp. 117–120.

[15] *IEEE Standard for Local and Metropolitan Area Networks—Part 15.6: Wireless Body Area Networks*, IEEE Standard 802.15.6-2012, IEEE Press, New York, NY, USA, Feb. 2012.

[16] X. Min, W. Xu, L. Wang, and G. Chen, "Promising performance of a frequency-modulated differential chaos shift keying ultra-wideband system under indoor environments," *IET Commun.*, vol. 4, no. 2, pp. 125–134, Jan. 2010.

[17] S. Chen, L. Wang, and G. Chen, "Data-aided timing synchronization for FM-DCSK UWB communication systems," *IEEE Trans. Ind. Electron.*, vol. 57, no. 5, pp. 1538–1545, May 2010.

[18] G. Kaddoum and E. Soujeri, "NR-DCSK: A noise reduction differential chaos shift keying system," *IEEE Trans. Circuits Syst. II, Exp. Briefs*, vol. 63, no. 7, pp. 648–652, Jul. 2016.

[19] W. K. Xu, L. Wang, and G. kolumbán, "A novel differential chaos shift keying modulation scheme," *Int. J. Bifurcation Chaos*, vol. 21, no. 3, pp. 799–814, Mar. 2011.

[20] H. Yang and G.-P. Jiang, "High-efficiency differential-chaos-shift-keying scheme for chaos-based noncoherent communication," *IEEE Trans. Circuits Syst. II, Exp. Briefs*, vol. 59, no. 5, pp. 312–316, May 2012.

[21] H. Yang and G.-P. Jiang, "Reference-modulated DCSK: A novel chaotic communication scheme," *IEEE Trans. Circuits Syst. II, Exp. Briefs*, vol. 60, no. 4, pp. 232–236, Apr. 2013.

[22] M. Herceg, G. Kaddoum, D. Vranješ, and E. Soujeri, "Permutation index DCSK modulation technique for secure multiuser high-data-rate communication systems," *IEEE Trans. Veh. Technol.*, vol. 67, no. 4, pp. 2997–3011, Apr. 2018.

[23] W. Xu, T. Huang, and L. Wang, "Code-shifted differential chaos shift keying with code index modulation for high data rate transmission," *IEEE Trans. Commun.*, vol. 65, no. 10, pp. 4285–4294, Oct. 2017.

[24] M. Herceg, D. Vranješ, G. Kaddoum, and E. Soujeri, "Commutation code index DCSK modulation technique for high-data-rate communication systems," *IEEE Trans. Circuits Syst. II, Exp. Briefs*, vol. 65, no. 12, pp. 1954–1958, Dec. 2018.

[25] G. Kaddoum, E. Soujeri, C. Arcila, and K. Eshteiwi, "I-DCSK: An improved noncoherent communication system architecture," *IEEE Trans. Circuits Syst. II, Exp. Briefs*, vol. 62, no. 9, pp. 901–905, Sep. 2015.

[26] H. Yang, G.-P. Jiang, and J. Duan, "Phase-separated DCSK: A simple delay-component-free solution for chaotic communications," *IEEE Trans. Circuits Syst. II, Exp. Briefs*, vol. 61, no. 12, pp. 967–971, Dec. 2014.

[27] C. Bai, H.-P. Ren, M. S. Baptista, and C. Grebogi, "Chaos-based underwater communication with arbitrary transducers and bandwidth," *Appl. Sci*, vol. 8, no. 2, p. 162, Jan. 2018.

[28] N. J. Corron, J. N. Blakely, and M. T. Stahl, "A matched filter for chaos," *Chaos, Interdiscipl. J. Nonlinear Sci.*, vol. 20, no. 2, Jun. 2010, Art. no. 023123.
[29] N. J. Corron and J. N. Blakely, "Chaos in optimal communication waveforms," in *Proc. Roy. Soc. A, Math., Phys. Eng. Sci.*, vol. 471, no. 2180, Aug. 2015, Art. no. 20150222.
[30] N. J. Corron, R. M. Cooper, and J. N. Blakely, "Analytically solvable chaotic oscillator based on a first-order filter," *Chaos, Interdiscipl. J. Nonlinear Sci.*, vol. 26, no. 2, Feb. 2016, Art. no. 023104.
[31] J. G. Proakis and M. Salehi, *Digital Communication*, 5th ed. New York, NY, USA: McGraw-Hill, 2008.
[32] J.-L. Yao, Y.-Z. Sun, H.-P. Ren, and C. Grebogi, "Experimental wireless communication using chaotic baseband waveform," *IEEE Trans. Veh. Techn.*, vol. 68, no. 1, pp. 578–591, Jan. 2019.
[33] J. N. Blakely, D. W. Hahs, and N. J. Corron, "Communication waveform properties of an exact folded-band chaotic oscillator," *Phys. D, Nonlinear Phenom.*, vol. 263, no. 22, pp. 99–106, Nov. 2013.
[34] N. J. Corron, J. N. Blakely, and M. T. Stahl, "A matched filter for chaos," *Chaos, Interdiscipl. J. Nonlinear Sci.*, vol. 22, May 2012, Art. no. 023123.

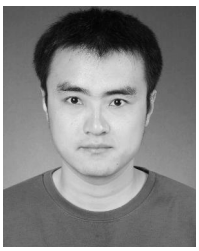

CHAO BAI was born in Xi'an, China, in 1988. He received the B.S. degree in automation from Xi'an Polytechnic University, in 2010, and the M.S. degree in control science and engineering from the Xi'an University of Technology, in 2014, where he is currently pursuing the Ph.D. degree.

His current research interests include chaotic communication and complex networks.

HAI-PENG REN (M'04) was born in Heilongjiang, China, in 1975. He received the Ph.D. degree in power electronics and power drives from the Xi'an University of Technology, in 2003.

He was a Visiting Researcher in the field of nonlinear phenomenon of power converters with Kyushu University, Japan, from 2004 to 2004. He has worked as a post Ph.D. Research Fellow in the field of time-delay system with Xi'an Jiaotong University, from 2005 to 2008. He was a Honorary Visiting Professor in the field of communication with chaos and complex networks with the University of Aberdeen, Scotland, from 2010 to 2011. Since 2008, he has been a Professor with the Department of Information and Control Engineering, Xi'an University of Technology, Xi'an, China. His fields include nonlinear system control, complex networks, and communication with nonlinear dynamics.

CELSO GREBOGI was born in Curitiba, Brazil, in 1947. He received the B.S. degree from the Universidade Federal do Parana, Parana, Brazil, in 1970, and the M.S. and Ph.D. degrees from the University of Maryland, College Park, MD, USA, in 1975 and 1978, respectively.

His current research focuses on systems biology, neurodynamics, methods to control chaos, the dynamics of spatio-temporal systems, active processes in chaotic flows, relativistic quantum dynamical systems, and nanosystems - including graphene and opto-mechanical systems.

Dr. Grebogi is a Fellow of the Royal Society of Edinburgh, a Fellow of the Brazilian Academy of Sciences, a Fellow of the World Academy of Sciences, a Fellow of the American Physical Society, and a Fellow of the Institute of Physics. As one of the participants, he has proposed the famous O. G. Y. method for chaos control. In addition, he was listed in the 2016 Thomson Reuters Citation Laureates.